

# 1D Tubular and 2D Metal–Organic Frameworks Based on a Flexible Amino Acid Derived Organic Spacer

Jean-Noël Rebilly, John Bacsá, and Matthew J. Rosseinsky\*<sup>[a]</sup>

*Dedicated to Professor C. N. R. Rao on the occasion of his 75th birthday*

**Abstract:** The organic ligand bgxH<sub>4</sub>, resulting from the condensation of two glutamate moieties on a xylene core, has been designed to generate chiral metal–organic frameworks with increased metal–metal distances in order to favor their potential porosity. The in situ reactivity of the ligand, through cyclization, led to the bpgxH<sub>2</sub> ligand,

which displays an extremely rich architectural potential. Under formate-generating conditions, two 1D tubular and one 2D MOFs based on bpgxH<sub>2</sub> have

**Keywords:** amino acids • chirality • encapsulated water • metal–organic frameworks • tubular structures

been obtained, incorporating up to three different organic linkers, and organized in an exquisite hierarchical way by the combined effects of the flexibility, the coordinating groups, and the H-bonding groups of the ligand. Furthermore, the tubular structures display pockets where water molecules are encapsulated.

## Introduction

Metal–organic frameworks (MOFs) have been the subject of an increasing number of studies over the last fifteen years.<sup>[1–4]</sup> The topology and internal surface functionality can be controlled by the choice of the metal ions and network-forming ligands. This synthetic approach thus permits the incorporation of specific properties within the material, such as magnetism,<sup>[5,6]</sup> luminescence,<sup>[7]</sup> chirality,<sup>[8,9]</sup> and catalytic centers.<sup>[10]</sup> The introduction of permanent porosity within these coordination polymer materials turned them into alternative candidates for applications ranging from separation and catalysis to gas storage,<sup>[11–14]</sup> with figures of merit that are competitive with zeolites in those fields.<sup>[15–17]</sup> The weaker framework-forming coordinate bonds in the MOF case permits synthesis under milder conditions compared with zeolites. This has a series of advantages — this paper addresses the assembly of homochiral networks from chiral building blocks and under relatively mild synthesis conditions, racemization of these units can be avoided, giving access to ho-

mo-chiral systems that can find applications in enantioselective separation and asymmetric catalysis, which remains a difficult goal to achieve with pure inorganic porous systems.<sup>[18,19]</sup>

Chiral MOFs can be crystallized from achiral building blocks,<sup>[20]</sup> but this generally leads to a racemate, thus limiting the possibility of enantioselective applications. Two main synthetic approaches can be used to generate homochiral porous frameworks. Porosity can be generated by means of an achiral organic spacer while chirality is located on an auxiliary chiral ligand.<sup>[21]</sup> A second strategy consists of using chiral organic spacer to introduce both properties within the framework.<sup>[10]</sup>

Naturally occurring chiral ligands are interesting starting materials as they are readily available in enantiopure form and on a gram scale. Several coordination polymers have been reported with natural chiral ligands.<sup>[22–25]</sup> As protein pockets play a crucial role in the selectivity of metalloenzymes, chiral aminoacids as ligands<sup>[24–37]</sup> are good candidates to generate enantioselectivity in porous MOFs. Aspartic acid was used to form the Ni(L-Asp)(bipy)<sub>0.5</sub> framework and a family of related derived systems.<sup>[27,28,38]</sup> Remarkable sorption enantioselectivity was observed in this porous chiral system, and channel dimensions could be tuned in one direction by the choice of the achiral 4,4'-bipyridine type linker. The other dimension is limited by the distance between the chiral centers which is set by the dimensions of the amino acid linker. In order to gain control over this dimension

[a] Dr. J.-N. Rebilly, Dr. J. Bacsá, Prof. M. J. Rosseinsky  
Department of Chemistry  
University of Liverpool  
Liverpool L69 7ZD (UK)  
Fax: (+44) 151-794-3587  
E-mail: m.j.rosseinsky@liv.ac.uk

Supporting information for this article is available on the WWW under <http://dx.doi.org/10.1002/asia.200900078>.

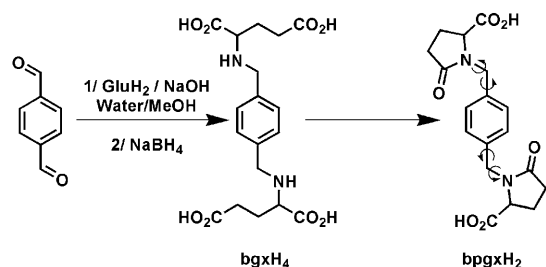
while retaining a ligand based on natural starting materials from the chiral pool, we adopted a related strategy to extend the pore dimensions, which are limited by the separation between the ligating groups of the amino acid, by using a network-forming ligand easily derived from amino acids by functionalizing them with a rigid aromatic separating platform. This paper will focus on the glutamic acid derivative, which displays a specific reactivity.

Herein, we report the synthesis of a chiral spacer derived from an amino acid and its use to generate framework structures. In the course of the reaction, the ligand undergoes internal cyclization, forming a chiral dicarboxylate ligand that generates 1D tubular structures with lanthanum and praseodymium and a 2D framework with copper and 4,4'-bipyridine. Furthermore, the solvent conditions used here allowed us to incorporate up to three different ligands in these structures by means of in situ generation of formate ions during the reaction.

## Results and Discussion

Ligand  $\alpha,\alpha'$ -bis(*N*-glutamyl)-*p*-xylene ( $\text{bgxH}_4$ ) was obtained from condensation of two equivalents of sodium glutamate and one equivalent of terephthalaldehyde in water/MeOH, followed by in situ reduction of imine bonds by sodium borohydride. This synthetic scheme generates a ligand which displays two amino acid moieties covalently linked by a xylene spacer core. Each amino acid moiety retains the coordination abilities of its original natural amino acid, the main difference being the nature of the amine function which is now secondary rather than primary in the natural amino acid. Metal-organic assemblies based on such ligands are thus expected to be less compact than their natural amino acid analogues. The presence of the xylene spacer between chiral centers imposes a minimum distance between metal centers, which is a key factor to generate porosity in these materials.

$\alpha,\alpha'$ -bis(*N*-pyroglutamyl)-*p*-xylene ( $\text{bpgxH}_2$ ) forms in situ during the solvothermal reaction with metal salts from cyclization of  $\text{bgxH}_4$  and was not isolated (Scheme 1). The  $\alpha$ -amino acid pattern disappears and  $\text{bpgxH}_2$  can be considered as a chiral dicarboxylic acid ligand, acting as a flexible spacer owing to its xylene core, and displaying H-bonding



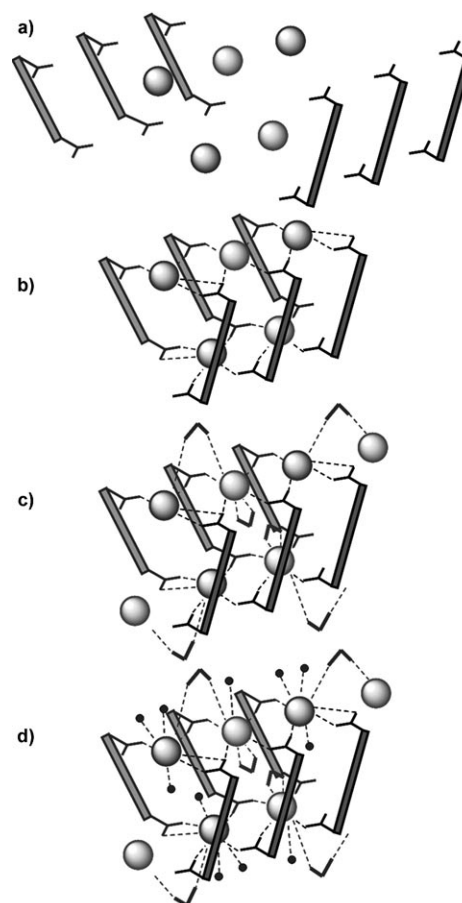
Scheme 1. Synthetic scheme for ligand  $\text{bpgxH}_2$ . Rotations about the  $\text{C}_{\alpha}-\text{C}_{\beta}$  and  $\text{C}_{\beta}-\text{N}$  bonds (curved arrows) are responsible for the relative orientation of the two carboxylate functions of  $\text{bpgxH}_2$ .

ability owing to the amide group generated during cyclization.

### Structural Description of 1–3

Reaction of lanthanum triflate with 0.75 equivalent of  $\text{bgxH}_4$  in Water/EtOH/DMF (v/v/v 2:3:3) at  $100^\circ$  for 18 h leads to very small white needles of  $[\text{La}(\text{bpgx})(\text{HCO}_2)(\text{H}_2\text{O})_2](\text{H}_2\text{O})_{1.5}$  **1**. **1** crystallizes in the chiral space group  $P2_1$  ( $a=9.5208$  (11) Å,  $b=17.6239$  (20) Å,  $c=26.8939$  (30) Å,  $\beta=100.195$ ).

The structure is made of tubular structures of  $[\text{La}(\text{bpgx})(\text{HCO}_2)(\text{H}_2\text{O})_2]$  oriented along the  $a$  direction and organized in the crystal by interstitial water molecules. The building of those tubes is explained in Scheme 2. They are made of two chains of La ions (Scheme 2 a). Those two chains are connected by two sets of  $\text{bpgx}^{2-}$  ligands in a ‘staple’ confor-



Scheme 2. Construction of the tubular structures. a) Views of the two chains of La ions (spheres) and the two sets of ‘staple-like’  $\text{bpgx}^{2-}$  ligands (rectangles). b) The carboxylates bridge the La ions to generate two chains that are connected by the organic backbone of the ligand represented as a rectangle (dark grey at the front, light grey at the back) to form the tubular structure. c) The formate ligands bridge metals on the outside of the tube (dark grey) and bind to La in a bidentate fashion inside the tube (light grey). They complete balancing the charge of La and make the structure neutral. d) the coordination sphere of La ions is completed by water molecules (dots).

mation where the two carboxylate groups are oriented in the same direction (Schemes 2a and 2b). The carboxylates bridge successive metal centers generating the two chains of La ions. The organic backbone of the ligands links the two chains to generate the metal–organic tube (Scheme 2b). To balance the charge of the metal, formate ions are present, bridging La ions on the outside of the tube, and bidentate to single La centers on the inside of the tube (Scheme 2c). Finally, water molecules complete the La coordination sphere (Scheme 2d). The inner formates are regularly spaced along the tube in such a way that they divide the tubular structure into pockets where two water molecules are encapsulated and held by a local H-bonding network involving coordinated water molecules. The asymmetric unit contains four non equivalent lanthanum ions. Two of these ions are eight coordinate (Figure 1a) and display the same type of coordination sphere (La1, La4) and two are nine coordinate (Figure 1b) with similar coordination environments (La2, La3). The coordination sphere is fully oxygenated in all cases. In the case of La1 and La4, the eight oxygen atoms come from one bidentate non-bridging formate function (2O), one bridging formate acting as a monodentate ligand (1O) towards La1 (or La4), four bridging carboxylate functions from four  $\text{bpgx}^{2-}$  ligands (1O each), and one water molecule (Figure 1c). They form a distorted square antiprismatic environment (Figure 1a). La2 and La3 are coordinated by one oxygen atom from a bridging formate, three oxygen atoms from three bridging carboxylate functions of  $\text{bpgx}^{2-}$  ligands (1O each), two oxygen atoms from a bridging carboxylate of a  $\text{bpgx}^{2-}$  ligand bound in a bidentate fashion (2O) and three water molecules. They are in a distorted tricapped trigonal prismatic geometry (Figure 1b).

The chains which make up the tubes consist of lanthanum centers with two alternating geometries along the chain axis. Each La1 ion is connected to two neighboring La3 ions by four bridging carboxylates from four  $\text{bpgx}^{2-}$  ligands, generating a chain structure based on alternating La1 and La3 (Figures 1c and 1d). The same pattern is observed for the (La2, La4) pair, generating a chain of alternating La2 and La4 (Figures 1c and 1d). Three of the  $\text{bpgx}^{2-}$  carboxylates bridge La1 and La3 (respectively La2 and La4) in a *syn anti* ( $\eta_1 \eta_1 \mu_2$ ) fashion (Figures 1c and 1d). The last one bridges them in a chelato-bridging ( $\eta_2 \eta_1 \mu_2$ ) mode. In order to balance the charge of the metal, a formate ion is present in the coordination sphere of each metal center. In the asymmetric unit, two of the formates act as bidentate non bridging (1,3) ligands towards La1 and La4 (Figure 1c). The other two are bridging ligands in a *syn syn* ( $\eta_1 \eta_1 \mu_2$ ) fashion, and connect La1a to only one of its neighbors (La3b via O4 and O3, but not La3a) on the one hand, and La4b to La2b (but not La2a) via O9, and O10 on the other hand. Water molecules complete the coordination sphere making La1 and La4 8 coordinate square antiprisms and La2 and La3 9 coordinate tricapped trigonal prisms. Most La–O bond lengths are between 2.415 and 2.605 Å. The chelato-bridging mode is the only mode that creates a shared corner between the two bridged La octahedra. All La ions are linked to each of

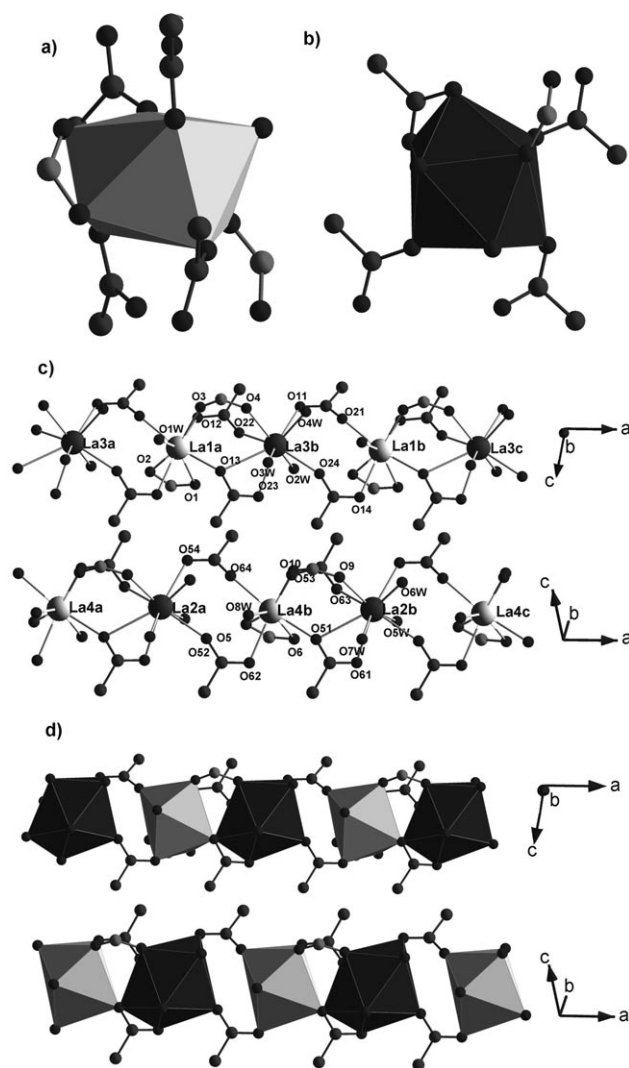


Figure 1. a) Polyhedron view of the square antiprismatic coordination sphere of La4 (similar for La1), showing the bending induced by the bidentate formate. b) Polyhedron view of the tricapped trigonal prismatic coordination sphere of La2 (similar for La3). Eight O atoms form a distorted square antiprism similar to the case of La4. The ninth atom (the second O atom of the bidentate carboxylate of  $\text{bpgx}^{2-}$ , on top) sits above the top square forming the summit of a square pyramid. c) Views of the 1D chains based on La1 and La3 ions (top), La2 and La4 ions (bottom), showing the coordination sphere of metal centers and the binding modes of the different carboxylate functions. d) Same views as in (c) with La polyhedral representation. Carboxylates from the  $\text{bpgx}^{2-}$  ligands are represented bearing one more C than formates. La1, La4: light grey; La2, La3: dark grey.

their two La neighbors in the chains by two  $\text{bpgx}^{2-}$  carboxylates. However, only one out of the four  $\text{bpgx}^{2-}$  carboxylates present in the coordination sphere is chelato-bridging, the other three are simply bridging. As a consequence, La polyhedra share one corner with only one of their two La polyhedra neighbors in the chains. They are thus grouped along the chains as pairs of corner-sharing polyhedra (Figure 1d).

The two 1D chains based on (La1, La3) and (La2, La4) are both oriented along the *a* axis of the structure (Figure 1c) and are connected together by the organic backbone

of the  $\text{bpgx}^{2-}$  ligands to lead to 1D tubular structures (Figures 2 and 3).

The  $\text{bpgx}^{2-}$  carboxylates define a pseudo-equatorial plane for La ions. The bridging formate ligands are located on the

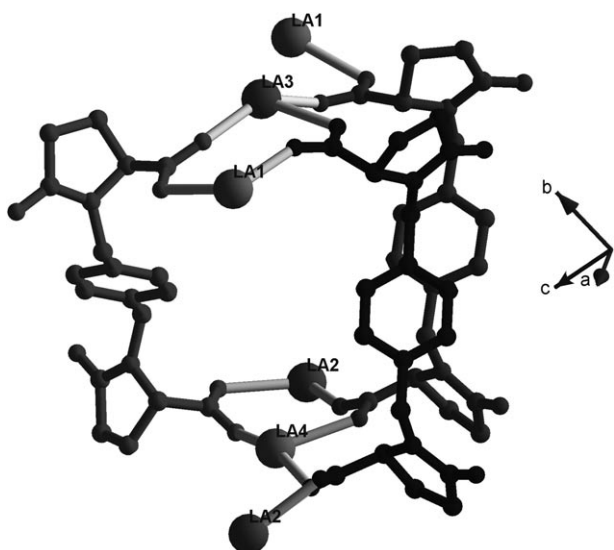


Figure 2. Partial view of a tubular structure in **1** showing the connectivity of the  $\text{bpgx}^{2-}$  ligands. Three different  $\text{bpgx}^{2-}$  ligands are highlighted in medium grey, dark grey, and black. They share a maximum of three metal centers. One of their carboxylate groups is involved in the bridging within the (La1, La3) chain, the other in the bridging within the (La2, La4) chain. The particular 'cis' conformation of  $\text{bpgx}^{2-}$  (carboxylates projecting in the same mean direction) limits the dimensionality to 1D. All other ligands are omitted for clarity.

external side of the tube. They occupy one coordination site on each La ion. The other external pseudo-axial sites are occupied by one (La1 and La4) or two (La2 and La3) of the oxygen atoms of water molecules (Scheme 2d, Figure 3b).

The pseudo-axial coordination sites on La1 and La4 located inside the tube are occupied by the two oxygen atoms of the bidentate chelating formates, while one water molecule sits on the pseudo-axial site of La2 and La3 (Scheme 2d, Figure 3).

In each  $\text{bpgx}^{2-}$  ligand, one of the carboxylate function is involved in the generation of the (La1, La3) chain and the other in the generation of the (La2, La4) one. The two carboxylate functions are oriented almost in the same mean direction and thus generate 1D tubular structures (Figures 2 and 3).

There are four different  $\text{bpgx}^{2-}$  ligands in the asymmetric unit. Two correspond to mode A (the two carboxylates are *syn anti* ( $\eta_1 \eta_1 \mu_2$ ) bridging, Scheme 3b), and two to mode B (one carboxylate is *syn anti* ( $\eta_1 \eta_1 \mu_2$ ) bridging, the second is chelato-bridging ( $\eta_2 \eta_1 \mu_2$ ), Scheme 3c).

Each  $\text{bpgx}^{2-}$  linker shares a maximum of three metal centers with another  $\text{bpgx}^{2-}$  linker (Figure 2). This arrangement of  $\text{bpgx}^{2-}$  ligands generates a tubular structure, with a pseudo-square cross-section, with two opposite edges based on the lanthanum ions and two pyroglutamate moieties of

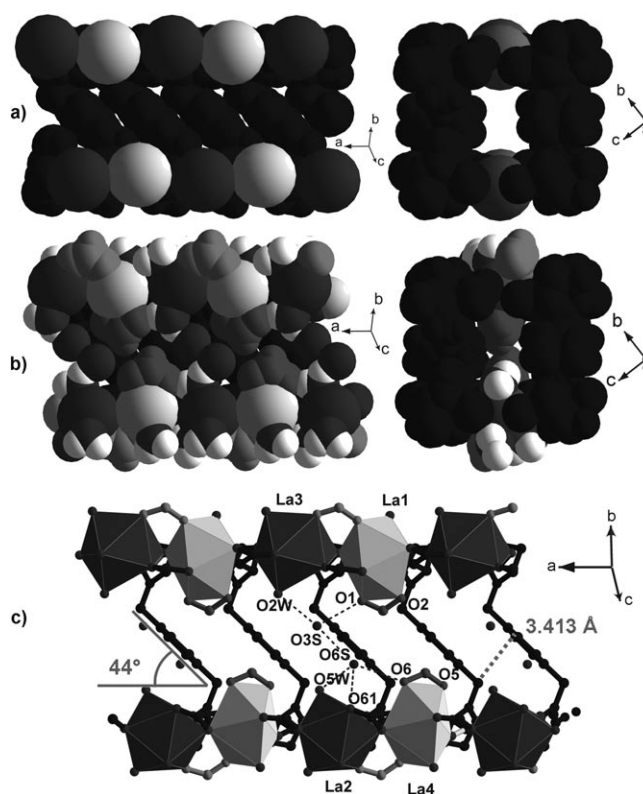
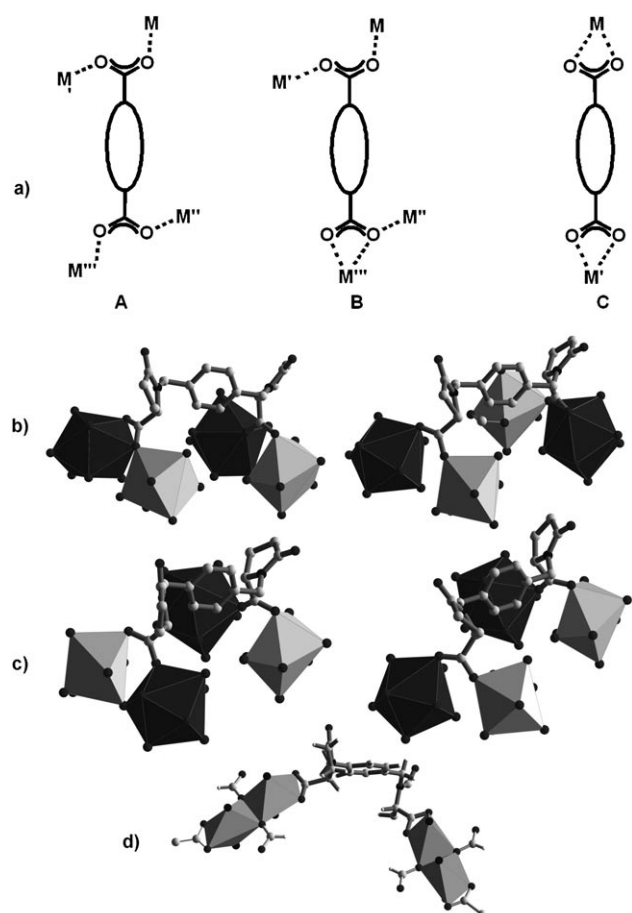


Figure 3. a) Views of the partial tubular structure formed by coordination of La to  $\text{bpgx}^{2-}$  linkers. Section of the tube in the (a, b+c) plane (left), cross section of the tube in the (b,c) plane (right).  $\text{bpgx}^{2-}$  linkers are depicted in black. All other ligands have been erased in these views. b) Views of the full tubular structure formed by coordination of La to  $\text{bpgx}^{2-}$  linkers (in black), formate ligands (outer ligands in light grey, inner ligands in medium grey), and water molecules. Section of the tube in the (a, b+c) plane (left), cross section of the tube in the (b,c) plane (right). The inner formates act as windows and divide the tube into pockets, that each encapsulate two water guest molecules, held by hydrogen bonding to the coordinated water molecules and formates present inside the tube. c) Polyhedral view of a tube (section of the tube in the (a, b+c) plane), showing the O atoms involved in the pockets hydrogen bonding network. The guest water molecules (O3S and O6S) interact essentially together (O3S–O6S=3.338 Å) and with the oxygen atoms of carboxylates (O3S–O1=3.338 Å, O6S–O61=3.256 Å, O6S–O6=3.393 Å) and coordinated water (O3S–O2W=2.594 Å, O6S–O5W=2.373 Å). La1 and La4 are light grey spheres, La2 and La3 are dark grey spheres. The oxygen atoms of the water molecules are depicted in dark grey, and hydrogen atoms are white.

$\text{bpgx}^{2-}$  ligands, and the other two edges corresponding to the xylene core of  $\text{bpgx}^{2-}$  (Figures 3a and 3b). The axis defined by the two benzylic C atoms of  $\text{bpgx}^{2-}$  forms a 44° angle with the *a* axis (Figure 3c).

The xylene moieties are twisted about their axis in such a way that they all stack along the *a* direction, creating CH– $\pi$  interactions between the aromatic ring of one  $\text{bpgx}^{2-}$  ligand and the xylene  $\text{CH}_2$  group of its neighbor. This conformation of the aromatic ring reduces the inner volume of the tube (Figures 3a and 3b). The channels arising from this tubular structure are partially obstructed by the inner ligands (Figure 3b). Indeed, the La1 and La4 ions that bear the bidentate formates on both sides of the inner surface of



Scheme 3. a) Binding modes of  $\text{bpgx}^{2-}$  ligands in compounds **1**, **2**, and **3**. The carboxylate groups are both *syn anti* ( $\eta_1 \eta_1 \mu_2$ ) bridging in type A ligands. In type B ligands, one function is *syn anti* ( $\eta_1 \eta_1 \mu_2$ ) bridging and the second is chelato-bridging ( $\eta_2 \eta_1 \mu_2$ ). In type C ligands, both functions are bidentate non-bridging. b) Type B ligands found in **1**. Left: one carboxylate is chelato-bridging and creates a pair of corner-sharing polyhedra, the other is simply bridging the two La ions belonging to another pair. Right: Again, one carboxylate creates a pair of corner-sharing polyhedra via the chelato-bridging mode, the other, simply bridging, links two La ions belonging to two different polyhedra pairs. c) Type A ligands found in **1**. None of the carboxylates is chelato-bridging: Thus, they don't create the polyhedra pairs. Left: one of the carboxylate connects two La ions belonging to the same pair of corner-sharing polyhedra, the other two La ions belonging to two different pairs. Right: both carboxylates connect two La ions belonging to different pairs. d) Type C ligands found in **3**. All  $\text{bpgx}^{2-}$  carboxylates are bidentate and non-bridging. La1, La4: light grey; La2, La3: dark grey; Cu: medium grey polyhedra; O: dark grey dots; C: medium grey; N: black.

the tubes, have coordinates along the  $a$  axis (tube axis) that are only separated by 2.237 Å. As a consequence, their formate ligands are very close to each other and tend to close the channels by dividing them into pockets (Figures 3b and 3c). This window pattern is repeated by a translation of  $a = 9.5208$  Å along the tube axis and leaves enough space in between to accommodate two water molecules (Figures 3b and 3c), which interact by hydrogen bonding with the coordinated water and, in a weaker way, with oxygen atoms of the coordinated carboxylates and with one another.

The tubular structures in **1** are all oriented along  $a$  in the crystal. Each tube has four nearest neighbor tubes. The mean plane formed by La ions of a tube is rotated by  $76^\circ$  about  $a$  with respect to the mean plane of its neighboring tubes (Figure 4a). The space between them is occupied by

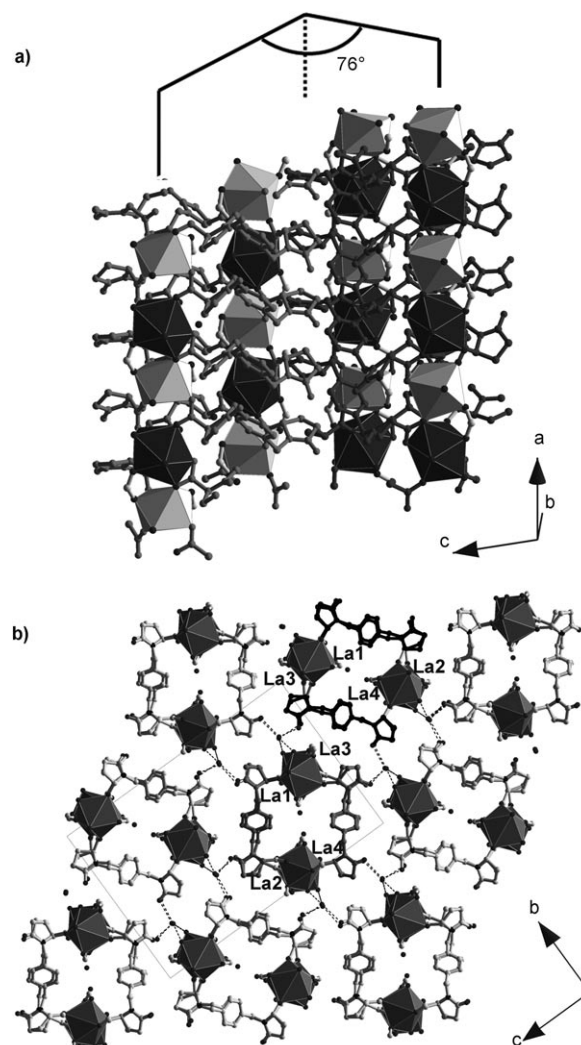


Figure 4. a) View of two neighboring tubes showing the  $76^\circ$  angle formed by the mean plane of their La ions. b) View along  $a$  of the packing of tubular structures in **1**. Two neighboring 1D substructures are highlighted in green and purple. Interstitial water molecules connect three tubes by hydrogen bonding to amide units and coordinated water molecules (highlighted in dotted lines).

water molecules (four per asymmetric unit). Each of them sits in a pseudo-tetrahedral environment and is interacting with three tubes through three hydrogen bonds involving water molecules coordinated to La on the first tube, and an oxygen atom of an amide function of  $\text{bpgx}^{2-}$  on each of the other two tubes (Figure 4b). The neutral amide bond, which does not bind metal centers unlike the charged carboxylates, is involved in the hydrogen bonding network and is thus responsible for the relative orientation of neighboring tubes resulting from their mutual hydrogen bonding to a set of

mediating water molecules. These amide functions, introduced in order to extend the amino acid core of the ligand, thus organize the tubes within the crystal, giving the network-forming ligand two roles stemming from the two different functional groups it supports.

A related compound **2** can be obtained in similar conditions by replacing lanthanum triflate by praseodymium nitrate in the procedure described for **1**. Structurally, **2** displays a building motif that is similar to the one described in Schemes 2a and 2b. However, unlike **1**, where formates balance the charge inside and outside the tubes (Scheme 2c), in the structure of **2**, the charge is balanced by three formates (two outside and one inside the tubes) for one nitrate (inside the tubes). Formally, one out of two inner formates is replaced by a nitrate in the structure of **2** and consequently reduces the inner volume of the tube's pockets (see the Supporting Information). Nevertheless, as evidenced by elemental analysis of the bulk material, this structure is not representative of the bulk phase, which corresponds, to a Pr equivalent to **1** (see the Supporting Information). Reaction of copper nitrate with one equivalent of  $\text{bgxH}_4$  and two equivalents of 4,4'-bipyridine in water/EtOH/DMF (v/v/v 2:3:3) at 100° for 18 h affords small blue crystals of  $[\text{Cu}(\text{bpgx})_{0.5}(\text{HCO}_2)(\text{bipy})](\text{H}_2\text{O})$  **3**. **3** crystallizes in the chiral space group  $P2_1$  ( $a=9.9916$  (64) Å,  $b=22.5295$  (141) Å,  $c=10.0941$  (62) Å,  $\beta=113.163$  (7)). **3** is remarkable as it is built from three distinct framework forming ligands —  $\text{bpgx}$  and  $\text{bipy}$  form an extended network from dimers bridged by formate. The asymmetric unit contains two crystallographically non equivalent copper ions, which however both play the same chemical role in forming the structure. Both are six coordinate and their coordination sphere is a distorted octahedron based on two oxygen atoms of a (1,3) bidentate carboxylate function of a  $\text{bpgx}^{2-}$  ligand, two nitrogen atoms from bipyridine ligands, and two oxygen atoms from two (1,1)  $\eta_2$  bridging formates. For both Cu1 and Cu2, the shortest bonds form a square plane made of the two pyridine nitrogen atoms sitting *trans* to each other (Cu1–N2=2.024 Å, Cu1–N1=2.025 Å, Cu2–N4=2.030 Å, Cu2–N5=1.965 Å, Figure 5a), one of the oxygen atoms of the bidentate carboxylate of  $\text{bpgx}^{2-}$  (Cu1–O1=1.943 Å, Cu2–O8=2.302 Å, Figure 5a), and the bridging oxygen atom of one of the bridging formates (Cu1–O4=1.981 Å, Cu2–O6=1.935 Å, Figure 5a). The O–Cu–N angles within those square planes are close to 90°, the highest deviations being N4–Cu2–O6=92.43° and N1–Cu1–O4=89.73°, and the O–Cu–O and N–Cu–N angles are confined above 168.57°. A fifth coordination site is occupied on one of the axial positions by the bridging oxygen atom of the formate that is not involved in the square planar coordination (O6 for Cu1, O4 for Cu2). The corresponding bonds are much longer than the equatorial ones ((Cu1–O6=2.332 Å, Cu2–O4=2.452 Å, Figure 5a), which can be attributed to the Jahn–Teller distortion along these directions. The final coordination site is occupied by the second oxygen atom of the bidentate carboxylate of  $\text{bpgx}^{2-}$  and is responsible for the main distortion with respect to the octahedral geometry, which is simultane-

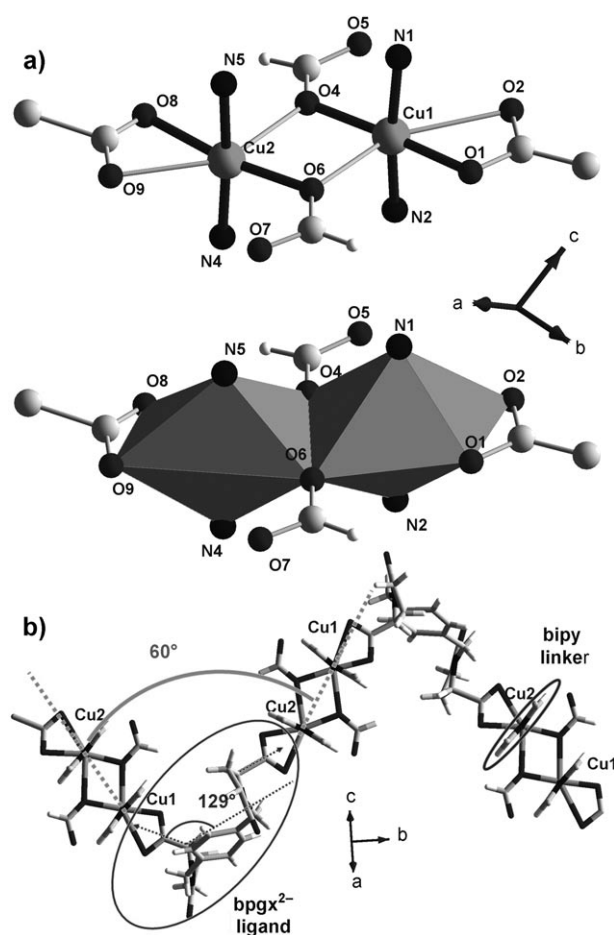


Figure 5. a) Views of the dimeric structure in **3** and the coordination sphere of the  $\text{Cu}^{2+}$  ions. Cu: medium grey, N: black, O: dark grey, C: light grey. Top: The shortest bonds forming a square plane and perpendicular to the Jahn–Teller axis of Cu are highlighted in bold dark grey. Bottom: Copper octahedra view showing the edge-sharing of the two Cu centers within the dimeric unit bridged by formate. b) View of three 1D substructures along the  $(a+c)$  direction, showing that each dimeric Cu unit is connected to two neighbors by  $\text{bpgx}^{2-}$  ligands and that each  $\text{bpgx}^{2-}$  ligand connects one Cu1 center to one Cu2 center. Along  $(a+c)$ , the angle between the carboxylate functions of  $\text{bpgx}^{2-}$  is 129°, while the angle formed by the mean plane of copper centers of two neighboring double chains is 60°.

ously an angular distortion and a bond length elongation (Figure 5a). This arises from the bite angle of the chelate carboxylate (O8–Cu2–O9=58.68°, O1–Cu2–O2=56.63°) that prevents coordination near the axial position. The sixth bonds are the longest of the coordination sphere (Cu1–O2=2.592 Å, Cu2–O9=2.410 Å). Atoms O4 and O6 are the bridging atoms of formates that bind metals in a (1,1)  $\eta_2$  mode. Each of them is involved in equatorial coordination on one site with a short bond and axial coordination on the other site with a longer bond arising from the Jahn–Teller elongation. As a consequence, the bridging is asymmetric and a dimeric structure based on a highly distorted diamond arrangement (Cu1–O4–Cu2–O6) is generated (Figure 5a). This structure can also be viewed as two edge-sharing octahedra, the shared edge being O4–O6.

The oxygen atoms of the formates, being bridging atoms in a diamond arrangement, define a common plane (Cu1–O4–Cu2–O6) for Cu1 and Cu2 that also includes all the other coordinating oxygen atoms (O8, O9, O1, O2, Figure 5a). Consequently, the Cu–N bonds of both Cu1 and Cu2 are perpendicular to this plane and thus parallel to each other. As the connectivity of 4,4'-bipyridine is linear, a one-dimensional substructure is generated by connecting the dimeric copper units with the bipy linker in the direction perpendicular to the (Cu1–O4–Cu2–O6) plane. Bipy linkers connect one Cu1 center to another Cu1, or one Cu2 center to another Cu2. This 1D Cu–bipy substructure is thus made of two parallel Cu–bipy chains, one made of Cu1 centers, the other of Cu2 centers, linked by the bridging formates (Figure 6a). The last two copper coordination sites that are

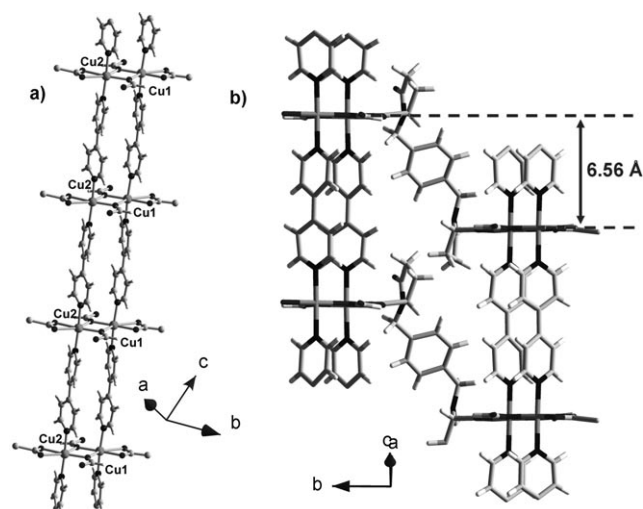


Figure 6. a) View of one double chain in **3** showing how two sets of bipy linkers connects the Cu1 and Cu2 centers into parallel chains bridged by formate. b) View of two neighboring bridged parallel chains in **3** showing the offset of 6.56 Å between them.

not involved in the formation of this double chain are occupied by the oxygen atoms of a bidentate carboxylate of  $\text{bpgx}^{2-}$  (O8 and O9 for Cu2 centers, O1 and O2 for Cu1 centers, Figure 5b). The second carboxylate of this  $\text{bpgx}^{2-}$  ligand binds a copper center of a neighboring chain of bipy-linked dimers in a similar manner ( $\text{bpgx}^{2-}$  adopts binding mode 'C', Schemes 3a and 3d, Figure 5b). They only act as terminal ligands to lock two coordination sites on each Cu center (Schemes 3a and 3d). The principal axes of all double chains are oriented along the same direction ( $a+c$ ) in the crystal structure. Consequently, each 1D substructure is connected to two neighbors by two sets of parallel  $\text{bpgx}^{2-}$  ligands. Each  $\text{bpgx}^{2-}$  ligand binds one Cu1 and one Cu2 center (Figure 5b). Each of the two carboxylate functions are included in a (Cu1–O4–Cu2–O6) plane (i.e., perpendicular to ( $a+c$ )). The distance between the planes of the two carboxylate functions of one  $\text{bpgx}^{2-}$  ligands (along ( $a+c$ )) is 6.56 Å. Within those planes, the directions of the two car-

boxylates of one  $\text{bpgx}^{2-}$  ligand form an angle of 129°. The conformation adopted by  $\text{bpgx}^{2-}$  in **3** is thus different from the 'cis' one observed in **1**. This will thus create an angle between the mean plane of the dimer pair of Cu ions of two neighboring 1D substructures linked by the bridging  $\text{bpgx}^{2-}$ . However, owing to the asymmetry of the bidentate binding mode of the carboxylate (one Cu–O bond is far longer than the other), this angle is only 60° and not the expected 129° (Figure 5b). Along the ( $a+c$ ) direction (principal axis), neighboring double chains displays an offset of 6.56 Å corresponding to the distance between the planes of the two carboxylate functions of  $\text{bpgx}^{2-}$  (Figure 6b). From a symmetry point of view, the arrangement of neighboring double chains linked by  $\text{bpgx}^{2-}$  ligands produces a  $2_1$  screw axis of space group  $P2_1$  along  $b$ .

The arrangement of double chains connected by  $\text{bpgx}^{2-}$  ligands generates a 2D structure of  $[\text{Cu}(\text{bpgx})(\text{HCO}_2)(\text{bipy})]$  that looks like a folded sheet due to the 60° angle formed by the mean plane of copper centers in neighboring double chains (Figure 5b). All sheets have a mean plane that is parallel to the ( $a+c, b$ ) plane. They are 'folded' along the ( $a+c$ ) direction, and the zone of folding is located on the aromatic ring of the  $\text{bpgx}^{2-}$  ligands (Figure 7). Neighboring sheets are generated by translation along  $a$  and  $c$ . They are thus piled up on top of one another in such a way that the convex part of one sheet fills the concave part of its neighbors, leaving a limited intersheet space (Figure 7a). Nevertheless, this space represents 12.8% of the cell volume. PLATON locates two voids per unit cell. They are located between the aromatic rings of  $\text{bpgx}^{2-}$  ligands belonging to two neighboring sheets and each account for 144 electrons (Figure 7b). This residual electronic density was attributed to solvent molecules (for water molecules only, it would correspond to  $14\text{H}_2\text{O}$  per unit cell). The presence of the oxygen atoms of the  $\text{bpgx}^{2-}$  amide bond and the formate ligand in the vicinity of the voids determined by PLATON suggests these functions are involved in hydrogen bonding with the interstitial water molecules and play a role in the organisation of sheets in the crystal.

### Synthesis and Characterisation

**1** can be obtained as a pure phase using a slightly different ratio of reagents and solvents than the one used to obtain the single crystals used in structure determination. Stoichiometric reaction of lanthanum triflate and  $\text{bgxH}_4$  in Water/EtOH/DMF (v/v/v 3:3:2) at 100° for 18 h leads to the isolation of **1** as a homogeneous solid made of very thin white needles. Phase purity is shown by a LeBail fit to powder X-ray diffraction data, indicating a single phase with cell parameters close to those of the single crystal determined at 150 K  $a=26.64323$  (78) Å,  $b'=17.71220$  (50) Å,  $c=9.04766$  (39) Å,  $\beta=97.69128$  (273) in space group  $P2_1$  (Figure S1 in the Supporting Information). The  $b'$  parameter is very close to the  $b$  parameter of the crystal structure.

Elemental analysis is in agreement with the crystal structure formula  $[\text{La}(\text{bpgx})(\text{HCO}_2)(\text{H}_2\text{O})_2](\text{H}_2\text{O})(\text{EtOH})_{0.33}$ .

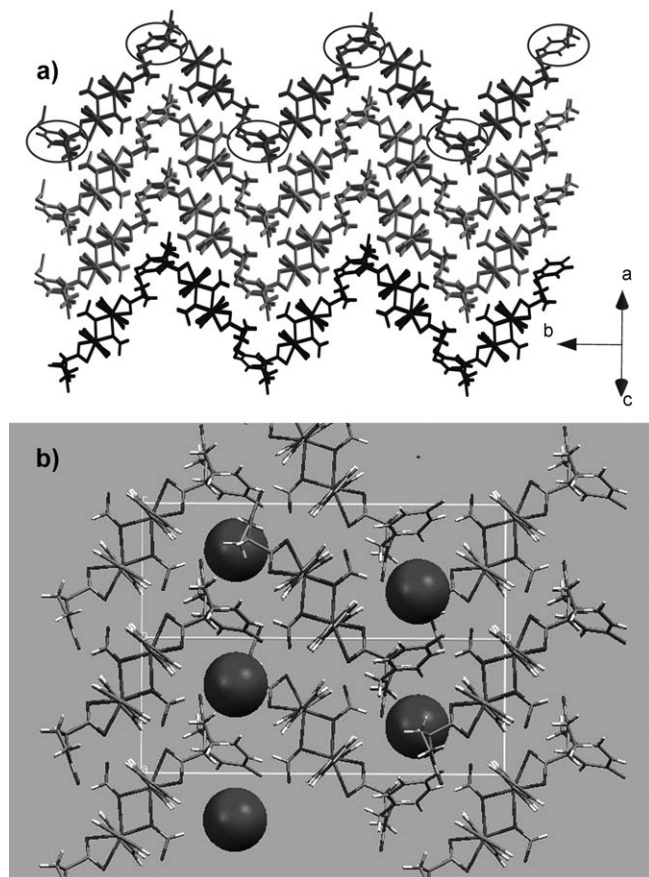


Figure 7. a) View of the packing of  $[\text{Cu}(\text{bpgx})(\text{HCO}_2)(\text{bipy})]$  sheets within the crystal structure of **3** along the  $(a+c)$  axis. Four different sheets are represented. The sheets are folded along  $(a+c)$  owing to the conformation of  $\text{bpgx}^{2-}$  ligands. The benzene rings of  $\text{bpgx}^{2-}$  ligands constitute the folding zone of the sheet (circled). b) View of the packing in **3**, showing the voids detected by PLATON (spheres), located between aromatic rings of  $\text{bpgx}^{2-}$  ligands belonging to two neighboring sheets.

TGA shows a weight loss of 8.2% centered around 125 °C (attributed to interstitial solvent and coordinated water situated outside of the tubes, 8.4% expected) and a smooth decrease of 3.3% between 125 °C and 340 °C (attributed to guest and coordinated water molecules inside the tubes, 2.94% expected) while the weight loss observed in the temperature range from 360 °C corresponds to the decomposition of **1** to  $\text{La}_2\text{O}_3$  (observed 60.2%, calculated 62%) (Figure S2 in the Supporting Information). **1** is thus a robust framework stable to 360 °C. After removal of the solvent at 100 °C overnight, the crystalline features of the powder pattern of **1** disappear and are replaced by a main broad peak centered around  $2\theta = 20.3^\circ$  ( $d$  spacing of 5.05 Å) and some smaller broad peaks, suggesting a loss of crystallinity while retaining some local order. After soaking the evacuated sample in water at room temperature for one day, the crystalline peaks characteristic for **1** reappear (Figure S3 in the Supporting Information).

**3** is obtained as a pure phase by reaction of copper nitrate with  $\text{bgxH}_4$  and 4,4'-bipyridine in the ratio  $\text{Cu}/\text{bgxH}_4/\text{bipy}$  1:1:2 in Water/EtOH/DMF v/v/v 3:3:2 at 100 °C for 18 h. **3** is

isolated as small blue crystals. Phase purity is evidenced by LeBail fit of the powder data (Figure S4 in the Supporting Information) which yields cell parameters,  $a = 10.22455$  (75) Å,  $b = 22.583$  (1) Å,  $c = 10.0612$  (8) Å,  $\beta = 113.724$  (3) in space group  $P2_1$ , which is very close to the cell obtained from single crystal diffraction.

Elemental analysis is in agreement with the crystal structure formula  $[\text{Cu}(\text{bpgx})_{0.5}(\text{HCO}_2)(\text{bipy})](\text{H}_2\text{O})$ . The first weight loss observed in TGA (Figure S5 in the Supporting Information), attributed to solvent loss, starts at room temperature up to 160 °C (observed 3%, calc. 3.9%) and is followed by a gradual decomposition to CuO between 180 °C and 500 °C (observed weight loss 79.3%, calculated from analysis formula 79%). The solvent content (one water molecule per copper) is significantly smaller than the one evaluated from the intersheet residual electronic density in the crystal structure. This is consistent with desolvation as soon as the crystals are removed from the mother liquor, as TGA shows a solvent loss starting at room temperature.

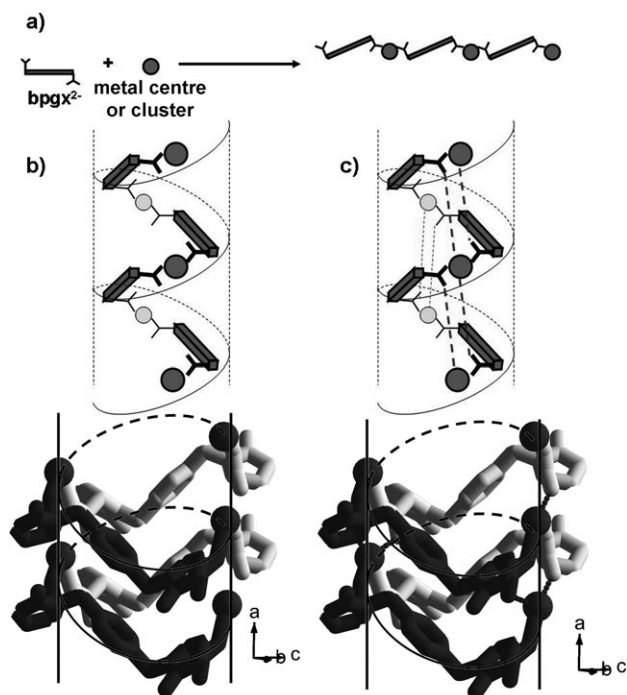
## Discussion

Amino acids as ligands display at least two potentially coordinating functions, the amino and the carboxylate groups, which usually coordinate to metals in a chelate binding mode generating a 5 membered ring. The carboxylate can become bridging within a coordination polymer, with the resulting 1,3 *syn-anti* bridging mode imposing a typical separation of 5.5 Å between connected metal centers. Further coordinating functions can be located on the side chain (as in the cases of cysteine and aspartic acid) extending the connectivity of the ligand and thus the dimensionality of the metal–organic framework. In order to introduce porosity within the framework, we synthesized spacers derived from amino acids by condensation of amino acids and terephthalaldehyde followed by in situ reduction. In this way, two chelating chiral sites are gathered in one ligand and separated by a xylene moiety, creating a distance of approximately 7.5 Å between the nitrogen atoms of the amino acids. A related approach has been used very recently to generate chiral ligands from amino-acids via the formation of an amide bond between terephthaloyl chloride and the amino group of aminoacids.<sup>[39]</sup> The approach described here retains the whole amino acid functionality on both sides of a terephthalic core. The glutamic acid derivative  $\text{bgxH}_4$  (Scheme 1) was thus reacted with different metal salts and neutral organic linkers to generate extended structures.

In the three structures reported here,  $\text{bgxH}_4$  undergoes in situ cyclization to generate  $\text{bpgxH}_2$ . This cyclization is a common feature of glutamic acid.<sup>[40]</sup> Pyroglutamic acid is generated by intramolecular reaction of the amino group with the carboxylic acid of the side chain of glutamic acid, forming an amide bond and a thermodynamically favored five membered ring. The reaction is catalyzed by Brønsted or Lewis acids. During the formation of **1**, **2**, and **3**, the metal probably acts as a Lewis catalyst to turn  $\text{bgxH}_4$  into  $\text{bpgxH}_2$  which can then react with the metal as a dicarboxy-

late ligand. The  $\text{bpgxH}_2$  ligand displays a flexible backbone. In particular, rotations about the  $\text{C}_{\text{Ar}}\text{--C}_{\text{CH}_2}$  and the  $\text{C}_{\text{CH}_2}\text{--N}$  bonds are responsible for the different relative orientations of the two carboxylate functions observed in **1**, **2**, and **3** (Scheme 1). A wide range of conformations are thus accessible, among which a pseudo 'cis' conformation, where the carboxylate functions are oriented along a similar mean direction, giving the ligand a 'staple' shape.

Coordination of  $\text{bpgx}^{2-}$  to metal centers can lead to extended linear 1D chain substructures as would be formed by any dicarboxylate ligand (Scheme 4a). However, the 'cis'



Scheme 4. a) Reaction of  $\text{bpgx}^{2-}$  with a metal generates a chain when the carboxylates act as monodentate ligands; b) This chain can coil on itself if  $\text{bpgx}^{2-}$  adopts the 'cis' conformation; c) This arrangement allows the formation of extra coordination bonds as the carboxylates become bridging which is impossible in the linear chain arrangement depicted in (a). b and c views: Top: The metal centers at the front are represented as large, dark spheres, those at the back are light grey; the bridging carboxylate M–O bonds are represented as dotted lines. Bottom: Case of **1**.  $\text{bpgx}^{2-}$  is highlighted in dark grey (front) and light grey (back). La is medium grey. The bridging M–O bonds are represented as thick dotted lines.

conformation in particular tends to favor the coiling of this 1D chain (Scheme 4b): Unlike the linear 1D arrangement, this coil arrangement allows every carboxylate function to become bridging, which is entropy favored (Scheme 4c). Indeed, if the 1D chain coils on itself and its carboxylates become bridging, coordinated solvent molecules will be substituted and released, leading to an increase in entropy. Furthermore, the encapsulated water molecules can act as templates for the formation of the coils, as they fit perfectly in the generated pockets and are held inside by H-bonding.

Those two aspects are probably the driving forces that favor the 'staple' conformation of  $\text{bpgx}^{2-}$  in **1** and **2**.

In the case of **3**, the ligand adopts a conformation where the carboxylates project away from each other and their orientations form an angle of  $129^\circ$ . This corresponds to the general situation depicted in Scheme 4a. In **3**, the metallic node is a formate-bridged dimeric copper unit and the substructure generated by coordination of  $\text{bpgx}^{2-}$  to these nodes is a chain (Figure 5b). Along ( $a+c$ ), the axes of the carboxylates form a high angle of  $129^\circ$ . They project away from each other (Figure 5b), preventing the structure from coiling on itself as in **1** and **2** (Scheme 4). This situation is probably the result of the lower coordination number of copper compared to lanthanides, as well as the presence in the reaction medium of ligands such as 4,4'-bipyridine that compete with the bridging mode of the carboxylate. The flexibility of  $\text{bpgx}^{2-}$  allows conformations in which the ligand can act either as a coil-generator (Scheme 4b, 4c) or as a spacer (Scheme 4a). The 'staple-conformation' of  $\text{bpgx}^{2-}$  observed in **1** and **2** generates the formation of a loop that brings metallic nodes in the vicinity of other carboxylates (Scheme 4b) and allows them to become bridging and extend the number of M–O bonds (Scheme 4c). It thus requires oxophilic metals that can access a high coordination number, typically lanthanides. The conformation of  $\text{bpgx}^{2-}$  observed in **3**, with a high angle between the directions of the two carboxylates, prevents this phenomenon and sees carboxylates acting as simple non-bridging ligands, with the presence of the bipy ligands organizing the carboxylate-bridged chains into higher order structures. It is thus adapted to transition metals with a lower coordination number, and a better affinity for nitrogen ligands. In those reaction conditions, lanthanides would thus tend to generate low dimensional structures, as the structure coils, to keep metal centers close to each other through bridging carboxylates. In the copper case,  $\text{bpgx}^{2-}$  carboxylates are bidentate non-bridging and keep metal centers away from each other in a 1D arrangement, leaving free sites in the coordination sphere to allow the framework to extend to other dimensions by means of a second linker. The use of bipy leads to the 2D structure of **3**. In all structures, the amide bond of  $\text{bpgx}^{2-}$  is not involved in coordination, but plays a crucial role in the way the 1D and 2D substructures are arranged within the crystal. In **1**, it organizes the tubular structures by an interstitial water molecule hydrogen-bonded to two amide oxygen atoms belonging to different tubes. In **3**, the presence of those functions in the vicinity of the 'solvent voids' suggests a similar organization. This ligand illustrates the fact that H-bonding interactions play a key role in the crystal generation.<sup>[41,42]</sup> The carboxylate functions of  $\text{bpgx}^{2-}$  generate metal–organic structures that are organized by a second functionality, the amide groups.

Nevertheless, the use of  $\text{bpgx}^{2-}$  allows us to constrain the distances between metal centers. Indeed, the 1D chain substructures of lanthanide ions in **1** and **2** or copper and bipyridine in **3**, are separated by the  $\text{bpgx}^{2-}$  ligand by 9.80 Å in **1**, 10.04 Å in **2**, and 9.55 Å in **3**. This validates our approach,

as this distance is, as expected, considerably increased with respect to the one induced by a single amino acid ligand (typically 5.5 Å).

Flexibility is a useful tool to generate various types of framework topologies. Nevertheless, it can decrease the crystallinity of materials. In the examples reported here, this is avoided by the presence of a secondary bidentate ligand, formate, which rigidifies the structure. Formates are not introduced directly in the reaction mixture. They are generated in situ from the hydrolysis of DMF. Indeed, the solvent mixture contains water and DMF, heated at 100°C, conditions harsh enough to hydrolyze DMF to formic acid and diethylamine. This has the advantage of slowly generating a base (HNEt<sub>2</sub>) and a secondary ligand (formate) during the course of the reaction. Attempts to generate **3** from the copper formate salt in water/methanol mixtures at the same temperature (100°C) led to a reported phase incorporating bipy but not bpgx<sup>2-</sup>. Formate is a small ligand, with versatile coordination (mono or bidentate), that is relatively rigid owing to its limited organic backbone. It can thus easily complete the coordination sphere of metal without steric hindrance, bridge metal centers, and rigidify the inorganic part of the system. In **1** and **2**, formate ligands display (1,3) ( $\eta_1 \eta_1 \mu_2$ ) *syn-syn* bridging modes on the outside of the tubes, improving the linkage between metals within the two lanthanide chains constituting each tube. They also act as bidentate non-bridging ligands inside the tubes, and thus only leave specific coordination sites accessible to bpgx<sup>2-</sup> carboxylates in the coordination sphere. When **1** and **2** are evacuated, the crystal structure peaks disappear, as solvent molecules organize the tubes with respect to one another by hydrogen bonding. Nevertheless, a broad peak replaces them (centered around a *d* spacing of 5.05 Å), which indicates that local ordering remains despite desolvation. The crystal structure peaks reappear when the evacuated solid is soaked in water, suggesting that the tube substructure is retained upon desolvation, and that rehydration restores the hydrogen bonding network responsible for their organization within the structure. This *d* spacing of 5.05 Å might be related to the distance between two metal centers bridged by the carboxylate groups of a bpgx<sup>2-</sup> ligand which in the solvated structures are between 4.608 Å and 4.945 Å in **1** and between 4.612 Å and 5.032 Å for **2** (Figure S12 in the Supporting Information).

In **3**, formates form the diamond-shaped Cu<sub>2</sub>O<sub>2</sub> core of the structure by a (1,1)  $\eta_2$  bridging mode. This motif locks two *cis* coordination sites on each Cu of the dimer and simultaneously locks the relative orientation of the coordination spheres of the two edge-sharing octahedral Cu centers. 4,4'-bipyridine tends to generate chain substructures and for this purpose locks two *trans* coordination sites on the axis perpendicular to the diamond-shaped Cu<sub>2</sub>O<sub>2</sub> core, leaving the bpgx<sup>2-</sup> carboxylates only the last two sites that sit *trans* to the formate oxygen atoms. The extended bridging rather than coil-forming *cis* conformation adopted by the bpgx ligand in **3** reflects the smaller and better-defined, more regular coordination sphere typically adopted by the transition

metal Cu in comparison with the lanthanides. The role of formate in all cases is to rigidify the inorganic structure by bridging metal centers and by locking specific coordination sites. In this manner, the flexibility of the framework is thus confined to the organic backbone of bpgx<sup>2-</sup> (by rotation about C<sub>Ar</sub>–C<sub>CH2</sub> and the C<sub>CH2</sub>–N bonds).

The reaction conditions used here, that gather the use of a flexible ligand and a formate-generating mixture of solvents, also allows us to incorporate up to three different organic linkers in the materials. Indeed, in all cases, two linkers, bpgx<sup>2-</sup> and formate, bridge ions and balance their charge. In the case of **3**, another neutral ligand is incorporated to further extend the dimensionality. This situation is not common. Most frameworks display a maximum of two organic linkers; either two charged linkers both balancing the charge of the metal<sup>[43,44]</sup> or one balancing the charge of the metal and the other neutral.<sup>[45–48]</sup> In some cases, an extra linker is present to enhance rigidity, in the form of an inorganic oxo or hydroxo bridge for instance, generating cluster nodes or more extended substructures.<sup>[11,49,50]</sup> Formate is an organic linker that plays a similar role, arising from its small size, its bridging ability, and its in situ formation during the synthesis of the framework.

## Conclusions

Three extended frameworks have been synthesized using a chiral spacer ligand derived from glutamic acid. The flexibility of the ligand backbone gives access to several topologies and dimensionalities depending on the type of metal center used in the synthesis. The reaction conditions produced in situ generation of formate ions, leading to 1D and 2D frameworks incorporating up to three different organic linkers. Formate ions also rigidify the inorganic architectures, giving access to coordination polymers where flexibility is mainly confined to the organic part of the framework. This synthetic strategy could be generalized to obtain open metal–organic frameworks from flexible ligands that are rigid enough to remain crystalline but that also display a certain degree of flexibility than could lead to properties such as guest-responsive behavior, gating processes, or kinetic trapping.<sup>[51]</sup>

## Experimental Section

### Single Crystal X-ray Diffraction

The single-crystal diffraction data were collected on station 9.8 of the Synchrotron Radiation Source at Daresbury Laboratory. Station 9.8 is a high flux single crystal facility which utilizes a Bruker-Nonius APEXII CCD area detector and D8 diffractometer at an X-ray wavelength of 0.6710 Å (**1**) and 0.6884 Å (**2**, **3**). Data were recorded at 150 K. The reflection data were integrated using APEX II software.<sup>[52]</sup> The data were corrected for absorption, decay and other systematic errors using SADABS V2008-1.<sup>[53]</sup> The structure was solved (by direct methods) and refined using SHELX-97.<sup>[54]</sup>

## Thermal Analysis

TGA data were recorded using a Seiko S-II instrument.

## X-ray Powder Diffraction

X-ray powder diffraction data were collected with  $\text{Co}_{\text{K}\alpha 1}$  radiation with a Panalytical X'pert Pro Multi-Purpose diffractometer in reflection geometry and  $\text{Cu}_{\text{K}\alpha 1}$  radiation with a Stoe Stadi-P diffractometer using a linear position sensitive detector.

## Synthesis

All reagents used in the ligand synthesis as well as  $(\text{CF}_3\text{SO}_3)_3\text{La}\cdot x\text{H}_2\text{O}$  and  $\text{Pr}(\text{NO}_3)_3\cdot 6\text{H}_2\text{O}$  were purchased from Sigma-Aldrich.  $\text{Cu}(\text{NO}_3)_2\cdot 3\text{H}_2\text{O}$  and solvents were purchased from VWR.

**$\alpha,\alpha'$ -bis(*N*-glutamyl)-*p*-xylene ( $\text{bgxH}_4$ ):** Glutamic acid (4 g, 27.2 mmol) was dissolved in an aqueous solution of sodium hydroxide (2 M, 20.4 mL). A solution of terephthalaldehyde (1.52 g, 11.34 mmol) in 60 mL of ethanol was added and the mixture was stirred at room temperature for 30 min, then cooled to 0 °C. Sodium borohydride (0.604 g, 15.9 mmol) was added in small portions and stirring was continued at room temperature for 90 min. A second portion of terephthalaldehyde (0.334 g, 2.5 mmol) was added, and the mixture was stirred for 20 min. Finally, a second portion of sodium borohydride (0.121 g, 2.9 mmol) was added and the suspension stirred for 45 min. The mixture was extracted with diethyl ether (2 × 50 mL) to remove excess terephthalaldehyde and the aqueous layer, diluted with 10 mL of water, was acidified at 0 °C to pH 2 by dropwise addition of concentrated HCl, at which point the compound precipitated as a white powder. The suspension was filtered, and washed with cold water. The white powder was then refluxed in ethanol for one hour, filtered again, and dried in air. Yield: 45%;  $^1\text{H NMR}$  ( $\text{bgxH}_4$ , 4 LiOH in  $\text{D}_2\text{O}$ ):  $\delta$  = 1.85 (m, 4H); 2.20 (t, 4H); 3.13 (t, 2H); 4.64 (d, 2H); 4.78 (d, 2H); 7.36 ppm (s, 4H);  $[\text{bgxH}_4](\text{H}_2\text{O})_{0.33}$ :  $M = 402.2$ ; elemental analysis: calcd (%) for  $\text{C}_{18}\text{H}_{24.66}\text{N}_2\text{O}_{8.33}$ : C 53.73, H 6.18, N 6.96; found: C 53.78, H 6.17, N 6.69.

**[La(bpgx)(HCO<sub>2</sub>)(H<sub>2</sub>O)<sub>2</sub>(H<sub>2</sub>O)<sub>1.5</sub> 1:** Lanthanum triflate (0.03 g, 0.05 mmol) and  $\text{bgxH}_4$  (0.020 g, 0.05 mmol) were mixed with 2 mL of water/EtOH/DMF (v/v/v 3:3:2) in a 12 mL scintillation vial and reacted at 100 ° for 18 h. The product crystallized as white needles that were filtered, washed thoroughly with water and ethanol and dried in air. Yield: 81%;  $[\text{La}(\text{bpgx})(\text{HCO}_2)(\text{H}_2\text{O})_2](\text{H}_2\text{O})(\text{EtOH})_{0.33}$ :  $M = 611.6$ ; elemental analysis: calcd (%) for  $\text{C}_{19.66}\text{H}_{27}\text{LaN}_2\text{O}_{11.33}$ : C 38.62, H 4.45, N 4.58, La 22.71; found: C 38.79, H 4.24, N 4.46, La 22.91. Single crystals suitable for X-ray diffraction were obtained from the reaction of lanthanum triflate (0.03 g, 0.05 mmol) and  $\text{bgxH}_4$  (0.015 g, 0.037 mmol) in 2 mL of water/EtOH/DMF (v/v/v 2:3:3) in a 12 mL scintillation vial and reacted at 100 ° for 18 h.

**[Pr(bpgx)(HCO<sub>2</sub>)<sub>0.75</sub>(NO<sub>3</sub>)<sub>0.25</sub>(H<sub>2</sub>O)<sub>2</sub>(H<sub>2</sub>O)<sub>1.5</sub> 2:** Praseodymium nitrate hexahydrate (0.022 g, 0.05 mmol) and  $\text{bgxH}_4$  (0.020 g, 0.05 mmol) were mixed with 2 mL of water/EtOH/DMF (v/v/v 3:3:2) in a 12 mL scintillation vial and reacted at 100 ° for 18 h. The product crystallized as white-greenish needles that were filtered, washed thoroughly with water and ethanol, and dried in air. Yield: 82%;  $[\text{Pr}(\text{bpgx})(\text{HCO}_2)(\text{H}_2\text{O})_{3.5}]$ :  $M = 607.3$ ; elemental analysis: calcd (%) for  $\text{C}_{19}\text{H}_{26}\text{PrN}_2\text{O}_{11.5}$ : C 37.57, H 4.31, N 4.61, Pr 23.20; found: C 37.86, H 4.12, N 4.88, Pr 22.88.

**[Cu(bpgx)<sub>0.5</sub>(HCO<sub>2</sub>)(bipy)](H<sub>2</sub>O) 3:** Copper nitrate trihydrate (0.018 g, 0.075 mmol),  $\text{bgxH}_4$  (0.030 g, 0.075 mmol) and 4,4'-bipyridine (0.024 g, 0.15 mmol) were mixed with 2 mL of water/EtOH/DMF (v/v/v 3:3:2) in a 12 mL scintillation vial and reacted at 100 ° for 18 h. The product crystallized as blue needles that were filtered, washed thoroughly with water and ethanol, and dried in air. Yield: 90%;  $[\text{Cu}(\text{bpgx})_{0.5}(\text{HCO}_2)(\text{bipy})](\text{H}_2\text{O})$ :  $M = 461.1$ ; elemental analysis: calcd (%) for  $\text{C}_{20}\text{H}_{20}\text{CuN}_3\text{O}_6$ : C 52.00, H 4.36, N 9.10, Cu 13.76; found: C 52.16, H 4.29, N 9.15, Cu 13.69. Single crystals suitable for X-ray diffraction were obtained from the reaction of copper nitrate trihydrate (0.048 g, 0.20 mmol),  $\text{bgxH}_4$  (0.040 g, 0.10 mmol), and 4,4'-bipyridine (0.032 g, 0.20 mmol) in 6 mL of water/EtOH/DMF (v/v/v 3:3:2) carried out in a 23 mL Teflon liner (Parr vessels) at 100 ° for 18 h.

## Acknowledgements

We thank the EPSRC for funding under EPSRC/C511794 and for access to the SRS, and the Leverhulme Trust for support of J.N.R. We thank the Royal Society for a Wolfson Research Merit Award to MJR.

- [1] B. F. Hoskins, R. Robson, *J. Am. Chem. Soc.* **1990**, *112*, 1546.
- [2] S. R. Batten, R. Robson, *Angew. Chem.* **1998**, *110*, 1558–1595; *Angew. Chem. Int. Ed.* **1998**, *37*, 1460–1494.
- [3] M. Eddaoudi, D. B. Moler, H. Li, B. Chen, T. M. Reinecke, M. O'Keeffe, O. M. Yaghi, *Acc. Chem. Res.* **2001**, *34*, 319–330.
- [4] O. R. Evans, W. Lin, *Acc. Chem. Res.* **2002**, *35*, 511–522.
- [5] M. Verdaguier, M. Julve, A. Michalowicz, O. Kahn, *Inorg. Chem.* **1983**, *22*, 2624–2629.
- [6] E. Pardo, D. Cangussu, M.-C. Dul, R. Lescouëzec, P. Herson, Y. Journaux, E. F. Pedroso, C. L. M. Pereira, M. C. Muñoz, R. Ruiz-García, J. Cano, P. Amorós, M. Julve, F. Lloret, *Angew. Chem.* **2008**, *120*, 4279–4284; *Angew. Chem. Int. Ed.* **2008**, *47*, 4211–4216.
- [7] G. F. De Sá, O. L. Malta, C. De Mello Donega, A. M. Simas, R. L. Longo, P. A. Santa-Cruz, E. F. Da Silva Jr, *Coord. Chem. Rev.* **2000**, *196*, 165–195.
- [8] W. Lin, *J. Solid State Chem.* **2005**, *178*, 2486–2490.
- [9] D. Bradshaw, T. J. Prior, E. J. Cussen, J. B. Claridge, M. J. Rosseinsky, *J. Am. Chem. Soc.* **2004**, *126*, 6106–6114.
- [10] J. S. Seo, D. Whang, H. Lee, S. I. Jun, J. Oh, Y. J. Jeon, K. Kim, *Nature* **2000**, *404*, 982–986.
- [11] M. Eddaoudi, J. Kim, N. Rosi, D. Vodak, J. Wachter, M. O'Keeffe, O. M. Yaghi, *Science* **2002**, *295*, 469–472.
- [12] X. Zhao, B. Xiao, A. J. Fletcher, K. M. Thomas, D. Bradshaw, M. J. Rosseinsky, *Science* **2004**, *306*, 1012–1015.
- [13] O. M. Yaghi, M. O'Keeffe, N. W. Ockwig, H. K. Chae, M. Eddaoudi, J. Kim, *Nature* **2003**, *423*, 705–714.
- [14] C. D. Wu, A. Hu, L. Zhang, W. Lin, *J. Am. Chem. Soc.* **2005**, *127*, 8940–8941.
- [15] U. Mueller, M. Schubert, F. Teich, H. Puetter, K. Schierle-Arndt, J. Pastre, *J. Mater. Chem.* **2006**, *16*, 626–636.
- [16] L. Alaerts, C. E. A. Kirschhock, M. Maes, M. A. Van der Veen, V. Finsy, A. Depla, J. A. Martens, G. V. Baron, P. A. Jacobs, J. F. M. Denayer, D. E. De Vos, *Angew. Chem.* **2007**, *119*, 4371–4375; *Angew. Chem. Int. Ed.* **2007**, *46*, 4293–4297.
- [17] L. Alaerts, E. Seguin, H. Poelman, F. Thibault-Starzyk, P. A. Jacobs, D. E. De Vos, *Chem. Eur. J.* **2006**, *12*, 7353–7363.
- [18] J. M. Newsam, M. M. J. Treacy, W. T. Koetsier, C. B. De Gruyter, *Proc. R. Soc. London Ser. A* **1988**, *420*, 375–405.
- [19] M. W. Anderson, O. Terasaki, T. Ohsuna, A. Phlippou, S. P. MacKay, A. Ferreira, J. Rocha, S. Lidin, *Nature* **1994**, *367*, 347–351.
- [20] T. Ezuhara, K. Endo, Y. Aoyama, *J. Am. Chem. Soc.* **1999**, *121*, 3279–3283.
- [21] C. J. Kepert, T. J. Prior, M. J. Rosseinsky, *J. Am. Chem. Soc.* **2000**, *122*, 5158–5168.
- [22] D. N. Dybtsev, A. L. Nuzhdin, H. Chun, K. P. Bryliakov, E. P. Talsi, V. P. Fedin, K. Kim, *Angew. Chem.* **2006**, *118*, 930.
- [23] S. Thushari, J. A. K. Cha, H. H. Y. Sung, S. S. Y. Chui, A. L. F. Leung, Y. F. Yen, I. D. Williams, *Chem. Commun.* **2005**, 5515–5517.
- [24] E. V. Anokhina, A. J. Jacobson, *J. Am. Chem. Soc.* **2004**, *126*, 3044–3045.
- [25] E. V. Anokhina, Y. B. Go, Y. Lee, T. Vogt, A. J. Jacobson, *J. Am. Chem. Soc.* **2006**, *128*, 9957–9962.
- [26] M. J. Ingleson, J. Bacsá, M. J. Rosseinsky, *Chem. Commun.* **2007**, 3036–3038.
- [27] R. Vaidhyanathan, D. Bradshaw, J. N. Rebilly, J. P. Barrio, J. A. Gould, N. G. Berry, M. J. Rosseinsky, *Angew. Chem.* **2006**, *118*, 6645–6649; *Angew. Chem. Int. Ed.* **2006**, *45*, 6495–6499.
- [28] M. J. Ingleson, J. Perez Barrio, J. Bacsá, C. Dickinson, H. Park, M. J. Rosseinsky, *Chem. Commun.* **2008**, 1287–1289.
- [29] L. Antolini, L. Menabue, G. C. Pellacani, G. Marcotrigiano, *Dalton Trans.* **1982**, 2541.

- [30] H. Schmidbaur, I. Bach, J. Riede, G. Muller, J. Helbig, G. Hopf, *Chem. Ber.* **1988**, 121.
- [31] T. H. Doayne, R. Pepinsky, T. Watanabe, *Acta Crystallogr.* **1957**, 10, 438.
- [32] Y. Zhang, M. K. Saha, I. Bernal, *CrystEngComm* **2003**, 5, 34.
- [33] M. Mizutani, N. Maejima, K. Jitsukawa, H. Masuda, H. Einaga, *Inorg. Chim. Acta* **1998**, 283, 105.
- [34] R. J. Flook, H. C. Freeman, M. L. Scudder, *Acta Crystallogr. Sect. B* **1977**, 33, 801.
- [35] C. M. Gramaccioli, *Acta Crystallogr.* **1966**, 21, 600.
- [36] Y. Yukawa, Y. Inomata, T. Takeuchi, *Bull. Chem. Soc. Jpn.* **1983**, 56, 2125.
- [37] Y. Xie, H.-H. Wu, G.-P. Yong, Z.-Y. Wang, R. Fan, R.-P. Li, G.-Q. Pan, Y.-C. Tian, L.-S. Sheng, L. Pan, J. Li, *J. Mol. Struct.* **2007**, 833, 88.
- [38] J. Perez Barrio, J.-N. Rebilly, B. Carter, D. Bradshaw, J. Bacsá, A. Y. Ganin, H. Park, A. Trewin, R. Vaidyanathan, A. I. Cooper, J. E. Warren, M. J. Rosseinsky, *Chem. Eur. J.* **2008**, 14, 4521–4532.
- [39] B. Wissler, A.-C. Chamayou, R. Miller, W. Scherer, C. Janiak, *CrystEngComm* **2008**, 10, 461.
- [40] G. N. Abraham, D. M. Podell, *Mol. Cell. Biochem.* **1981**, 38, 181–190.
- [41] C. J. Kepert, T. J. Prior, M. J. Rosseinsky, *J. Solid State Chem.* **2000**, 152.
- [42] T. J. Prior, M. J. Rosseinsky, *Chem. Commun.* **2001**, 1222–1223.
- [43] K. Koh, A. G. Wong-Foy, A. J. Matzger, *Angew. Chem.* **2008**, 120, 689–692; *Angew. Chem. Int. Ed.* **2008**, 47, 677–680.
- [44] W. Chen, J.-Y. Wang, C. Chen, Q. Yue, H.-M. Yuan, J.-S. Chen, S.-N. Wang, *Inorg. Chem.* **2003**, 42, 944–946.
- [45] T. K. Maji, K. Uemura, H. C. Chang, R. Matsuda, S. Kitagawa, *Angew. Chem.* **2004**, 116, 3331–3334; *Angew. Chem. Int. Ed.* **2004**, 43, 3269–3272.
- [46] C. Ruiz-Pérez, P. Lorenzo-Luis, M. Hernandez-Molina, M. Milagros Laz, F. S. Delgado, P. Gili, M. Julve, *Eur. J. Inorg. Chem.* **2004**, 3873–3879.
- [47] E.-Y. Choi, K. Park, C.-M. Yang, H. Kim, J.-H. Son, S. W. Lee, Y. H. Lee, D. Min, Y.-U. Kwon, *Chem. Eur. J.* **2004**, 10, 5535–5540.
- [48] R. Matsuda, R. Kitaura, S. Kitagawa, Y. Kubota, T. C. Kobayashi, S. Horike, M. Takata, *J. Am. Chem. Soc.* **2004**, 126, 14063–14070.
- [49] J. Jia, X. Lin, C. Wilson, A. J. Blake, N. R. Champness, P. Hubberstey, G. Walker, E. J. Cussen, M. Schröder, *Chem. Commun.* **2007**, 840–842.
- [50] M. Latroche, S. Surble, C. Serre, C. Mellot-Draznieks, P. L. Llewellyn, J. H. Lee, J. S. Chang, H. J. Sung, G. Férey, *Angew. Chem.* **2006**, 118, 8407–8411; *Angew. Chem. Int. Ed.* **2006**, 45, 8227–8231.
- [51] A. J. Fletcher, K. M. Thomas, M. J. Rosseinsky, *J. Solid State Chem.* **2005**, 178, 2491–2510.
- [52] Bruker, *APEX II*, Bruker AXS Inc., Madison, Wisconsin, USA, **2005**.
- [53] Bruker, *SADABS Version 2008-2*, Bruker AXS Inc., Madison, Wisconsin, USA, **2007**.
- [54] G. M. Sheldrick, *SHELX97*, University of Göttingen, Germany, **1997**.

Received: February 22, 2009  
Published online: May 4, 2009